

Cite this: *Dalton Trans.*, 2024, **53**, 10446Received 15th April 2024,
Accepted 24th May 2024

DOI: 10.1039/d4dt01112k

rsc.li/dalton

A Bis(silylene)silole – synthesis, properties and reactivity†

Chenghuan Liu, Marc Schmidtman and Thomas Müller*

A 1,1-bis(silylene)silole has been synthesised by a double salt-metathesis reaction from potassium silacyclopentadienediide, $K_2[1]$, and an amidinato-stabilized silylene chloride in a 1 : 2 ratio. The red colour of the title compound is due to the $lp(Si)/\pi^*(silole)$ transition. This band is bathochromically shifted compared to that of other 1,1-bissilylsiloles suggesting enhanced conjugation between the silole π -system and the newly formed $Si(II)-Si(IV)-Si(II)$ group. The bissilylene is easily oxidised by the elemental chalcogens S, Se, and Te and forms a bissilaimide by reaction with an arylazide.

Introduction

Siloles and amidinato silylenes represent important branches in the growing tree of organosilicon chemistry. The unique photophysical properties of siloles and their derivatives have opened new perspectives for materials science.¹ The discovery of the aggregation induced emission (AIE) effect is here only one of the most prominent developments.² Amidinato silylenes with tricoordinated silicon atoms show unique nucleophilic properties. Since the first report on their synthesis by H. Roesky and coworkers in 2006,³ their use as stabilizing ligands in main group and transition metal chemistry has strongly influenced the area of small molecule and bond activation.^{4–7} In this respect the work of Driess and coworkers is of particular interest.^{8–13} This group developed a series of bissilylenes A–G (Fig. 1)^{11,14–19} that show interesting cooperative reactivity that is useful for the synthesis of unusual main group compounds and makes these compounds valuable ligands in coordination chemistry. The groups of So and Roesky/Stalke added to this series bissilylenes H and J.^{20,21} In these two examples the silylenes are separated by tetracoordinated silicon atoms and the resulting Si–Si bonds are unusually long (241–245 pm). This suggests relatively small Si–Si bond energies and therefore small separations between σ - and σ^* -orbitals with favourable preconditions for σ -conjugation.²² Before the background of these considerations, our motivation to combine the silole group with tricoordinated amidinato sily-

lenes was twofold. We were interested in the influence of the two $Si(II)$ substituents on the electronic situation of the silole ring and we were curious to study whether cooperative reactivity between the two nucleophilic $Si(II)$ centres is possible when held together by the silole group.

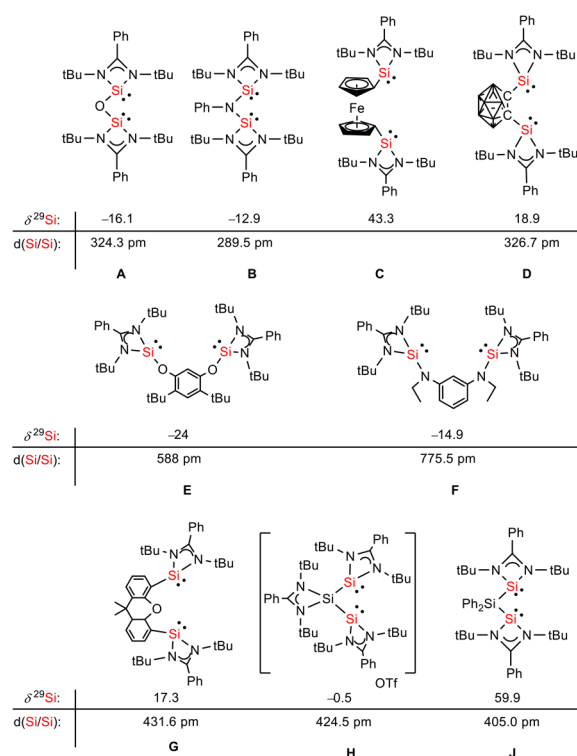


Fig. 1 Examples of chelating bis(silylene) ligands A–J, their ^{29}Si NMR chemical shifts, $\delta^{29}Si$, and their Si/Si separation, $d(Si/Si)$.

Institut für Chemie, Carl Ossietzky Universität Oldenburg, Carl von Ossietzky-Str. 9-11, 26129 Oldenburg, Federal Republic of Germany, European Union.

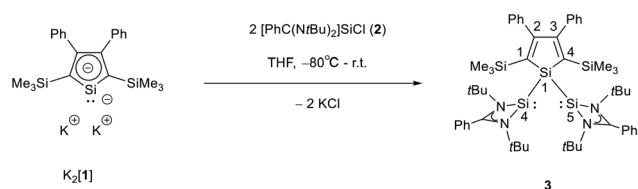
E-mail: thomas.mueller@uni-oldenburg.de

† Electronic supplementary information (ESI) available. CCDC 2345912–2345916. For ESI and crystallographic data in CIF or other electronic format see DOI: <https://doi.org/10.1039/d4dt01112k>



Results and discussion

The starting materials of choice were silole dianions $[1]^{2-}$ and amidinate-stabilized silylene chloride $\text{RSi}(\text{:})\text{Cl}$ ($\text{R} = \text{PhC}(\text{N}t\text{Bu})_2$), **2**.^{3,23} Treatment of dipotassium silacyclopentadiene-diene $\text{K}_2[1]$ with silylene chloride **2** in a molar ratio of 1 : 2 in THF gives the expected bis(silylene)silole **3** in 65% yield (Scheme 1). The formation of silole **3** was confirmed by NMR spectroscopy. The ^1H NMR spectrum of silole **3** reveals two singlets, one for the *t*Bu groups and one corresponding to the trimethylsilyl groups, as well as one set of resonances for the phenyl groups of the amidinate ligand and of the silole ring (see the ESI†). In the ^{29}Si NMR spectrum, three signals were detected at $\delta^{29}\text{Si} = -10.6$, 6.5, and 65.6, which were assigned to the trimethylsilyl group, the silole (Si1) and silylene silicon atoms (Si4, Si5), respectively. The assignment is supported by the detection of a $^1J(\text{Si1}-\text{Si4/5})$ coupling constant of 62 Hz for the two resonances at high frequencies. The ^{29}Si NMR resonance of the silylene silicon atoms Si4/5 appears downfield shifted from those of the starting material, amidinato silylene chloride **2** ($\delta^{29}\text{Si} = 14.6$),³ but in the same chemical shift region as those of the tris(trimethylsilyl)-substituted benzamidinato silylene **6** and the diphenylsilylene separated bis(silylene) **J** (Fig. 1 and 2),²⁴ confirming the deshielding effect of the silicon substituent for this class of silylenes. While the silole silicon atom is strongly shielded by $\Delta\delta^{29}\text{Si} = -142$ compared to that of $\text{K}_2[1]$ ($\delta^{29}\text{Si} = 148.5$),²³ its ^{29}Si NMR resonance appears low field shifted compared to disilyl-substituted siloles, such as bis(silyl)silole **5** ($\delta^{29}\text{Si} = -17.1$).²⁵ The origin of the red colour of a solution of silole **3** in *n*-hexane is a long wave absorption



Scheme 1 Synthesis of silole bridged bis(silylene) complex **3**.

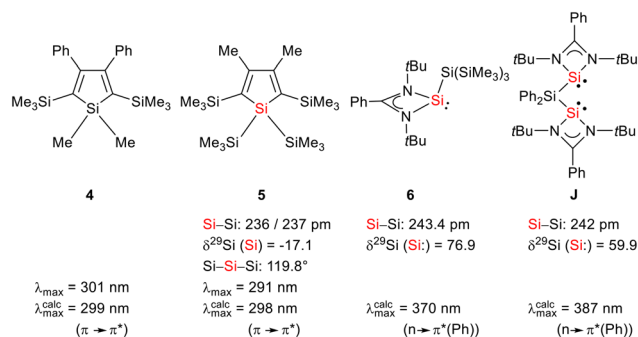


Fig. 2 Structural and spectroscopic data of selected siloles and silicon (ii) amidinates.

band at $\lambda = 474$ nm. In contrast, structurally strongly related siloles such as 1,1-dimethylsilole **4** and 1,1-bis(trimethylsilyl)silole **5** are colourless and show long-wave absorptions in the near UV-region (Fig. 2).²⁶ The colours of crystals of tris(trimethylsilyl)silyl substituted amidinato silylene **6** and of bis(silylene) **J** are yellow, which suggests an absorption band around 400 nm.^{21,24} This is in qualitative agreement with calculated long-wave UV-absorption bands at $\lambda_{\text{max}} = 370$ nm (**6**) and at $\lambda_{\text{max}} = 387$ nm (**J**) (M06-2X/6-311+G(d,p), Fig. 2).^{27,28} This comparison indicates that the combination of the silole ring with two amidinato silylene substituents leads to a significant bathochromic shift of the long-wave absorption in bis(silylene)silole **3**.

Red crystals of bis(silylene)silole **3** suitable for single crystal X-ray diffraction (sc-XRD) analysis were obtained from a saturated Et_2O solution at 5 °C and its molecular structure is pictured in Fig. 3. The central silacyclopentadiene ring shows the expected planar structure (the distance of Si1 from the least square plane of the four carbon atoms is 1.9 pm) with a short/long/short C-C bond length variation of the butadiene part and regular Si1-C1 and Si1-C4 bond lengths (Fig. 2). The silicon atom Si1 is tetracoordinated and the plane spanned by Si1 and the two silylene silicon atoms Si4 and Si5 is almost orthogonally oriented to the silole ring (the dihedral angle between both planes is 80.7°). The Si-Si bonds are long (245.9 and 246.3 pm) compared to exocyclic Si-Si bonds in siloles (e.g. silole **5**)²⁵ but are in the expected region for exocyclic Si-Si bonds of amidinate-stabilized silylenes (e.g. silylene **6** and bis(silylenes) **H** and **J** (Si-Si = 240–245 pm)).^{20,24} The Si4-Si1-Si5 bond angle is 108.9°, close to the ideal tetrahedral angle. The coordination environment of the two tricoordinated silicon atoms Si4 and Si5 is trigonal pyramidal (sum of the bond angles α : $\sum\alpha(\text{Si4}) = 281.1^\circ$ and $\sum\alpha(\text{Si5}) = 284.3^\circ$), which is consistent with the presence of a stereoactive lone pair at each silicon centre. The separation between both tricoordinated silicon atoms is 400.5 pm, in the range of related Si/Si dis-

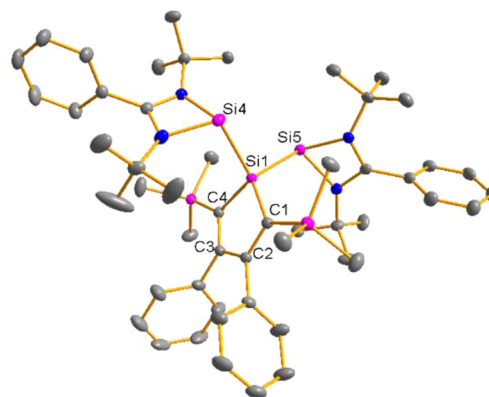


Fig. 3 Molecular structure of bis(silylene)silole **3** in the crystal (hydrogen atoms are omitted; thermal ellipsoids at 50% probability). Selected atom distances [pm] and angles [°]: Si1-Si4 245.90(6), Si1-Si5 246.35(5), Si1-C1 189.11(17), Si1-C4 189.48(15), C1-C2 137.09(22), C2-C3 147.64(23), C3-C4 137.26(19), Si4-Si1-Si5 108.91(19).



tances in bisilylenes **A–E** and **G–J** (326–588 pm) (Fig. 1). The amidinate rings are oriented in an *anti*-configuration with regard to the Si₄Si₁Si₅ plane. Therefore, the lone pairs at the silylene silicon atoms point in opposite directions.

This is supported by the results of quantum mechanical calculations at the M06-2X/6-311+G(d,p) level of theory.²⁷ The molecular structure of silole **3** at this level of theory agrees well with data that was obtained from XRD analysis. The smallest deviation between important structural parameters is less than 2% (see the ESI†). This good agreement allows a closer inspection of the electronic situation in bisilylene silole **3** by this DFT method. The HOMO–2 is dominated by contributions of the highest π -orbital of the butadiene part of the silole ring (Fig. 4). As expected, the HOMO and HOMO–1 are combinations of the lone pairs at the tricoordinated silicon atoms with significant contributions of the σ -Si–Si bonds (see Fig. 4) with the lone pairs pointing in opposite directions. As is typical for siloles, the LUMO is a combination of the π^* orbitals of the butadiene part of the silole ring and the σ^* -Si–Si bonds (π^*/σ^* conjugation).²⁹ Different to other siloles (e.g. **4** and **5**, Fig. 2 and the ESI†) the long wave transition is a lp(Si)/ π^* (silole) transition. The HOMO/LUMO energy gap is relatively small (2.18 eV) and the lowest absorption band, which is assigned to the HOMO/LUMO transition, is calculated at 425 nm (M06-2X/6-311+G(d,p)), close to the experimental value of 474 nm. Therefore, the substitution of the silole ring with two tricoordinated silylenes leads to a change in the nature of the long wave absorption and to a significant bathochromic shift.

We investigated the reactivity of several transition metal complexes (such as Fe(0), Ni(0), Ni(II), Pd(0), Pd(II), Au(I), and Zn(II) complexes) applying different conditions and stoichiometries to probe the coordination ability of silole **3**. However, in all investigated cases the reaction was not selective, and we

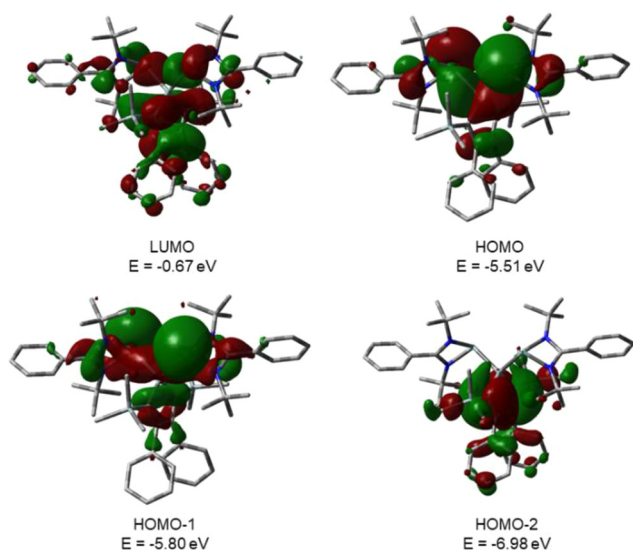
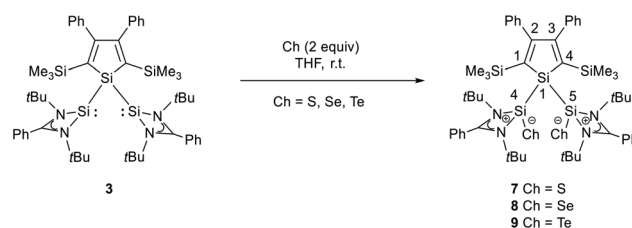


Fig. 4 Calculated surface diagrams of molecular orbitals of bisilylene silole **3** (M06-2X/6-311+G(d,p), isodensity value 0.02).

were not able to isolate a metal complex of bis(silylene)silole **3**. The reason for this failure is not clear but the unfavourable *anti*-orientation of the two silylene groups in the conformational ground state might contribute. Due to the lack of defined reactivity *versus* metal complexes, we tested the reactivity of bis(silylene)silole **3** *versus* standard reagents such as elemental chalcogens (Scheme 2) and arylazides (Scheme 3).

As expected bis(silylene)silole **3** is unstable in air and the controlled reactions with dioxygen (air) or oxygen atom donors (dinitrogen monoxide) are not selective. In contrast, two equivalents of the heavier chalcogens sulphur, selenium and tellurium react smoothly with silole **3** in THF at room temperature to yield the dichalcogenides **7–9** in acceptable to good yields (66–83%, Scheme 2). The identity and structure of these compounds were confirmed by NMR spectroscopy and sc-XRD. The ²⁹Si NMR spectra of chalcogenides **7–9** display for the silylene silicon atom signals at $\delta^{29}\text{Si} = 19.7$ (**7**), 15.0 (**8**), and -11.7 (**9**), which show the expected low frequency shift going from sulphide to telluride known for tetra- and pentacoordinated silicon chalcogenides.^{24,30–32} These ²⁹Si NMR signals are in the typical region of tetracoordinated amidinate stabilized silicon chalcogenides bracketed by the values for the corresponding hypersilyl- and bisilylamino-substituted chalcogenides **13** and **14** (see Fig. 5).^{24,33} Compared to tricoordinated silicon chalcogenides (heavy silaketones) such as **10–12**, the ²⁹Si resonances of **7–9** are significantly shifted to lower frequencies^{34–39} but they are clearly distinguished from those of the pentacoordinated silicon chalcogenides **16** (Fig. 5).³¹ Based on this assessment of the ²⁹Si NMR chemical shifts, we place the electronic effects of the silole ring in chalcogenides **7–9** between the electron donating hypersilyl group (in **13**) and the electronegative amino substituent (in **14**) or the even more electronegative phenoxy substituent in the bis(silicon chalcogenide) **15**.^{24,30,33} The silicon selenide **8** shows Si/Se satellites that are separated by ¹J(SiSe) = 292 Hz, in the typical range for tetracoordinated silicon selenides (e.g. 284 Hz (**14b**); 247 Hz in Ter*(H)(Me₄Im) Si(Se), Ter* = 2,6-bis-(2,4,6-triisopropylphenyl)phenyl) and significantly larger than is found for silylselenoethers such as (Me₃Si)₂Se (¹J_{SiSe} = 107 Hz).^{32,33} In addition, the ²⁹Si NMR data gives no indication of any intramolecular interaction between the two SiCh groups.

The silicon selenide **8** exhibits a resonance in the ⁷⁷Se{¹H} NMR spectrum at $\delta^{77}\text{Se} = -184.3$ and the telluride **9** is characterized by one signal at $\delta^{125}\text{Te} = -692.5$ in the ¹²⁵Te{¹H} NMR spectrum. This is for both nuclei a significant shift to low fre-



Scheme 2 Reaction of bis(silylene)silole **3** with chalcogens S, Se, and Te.



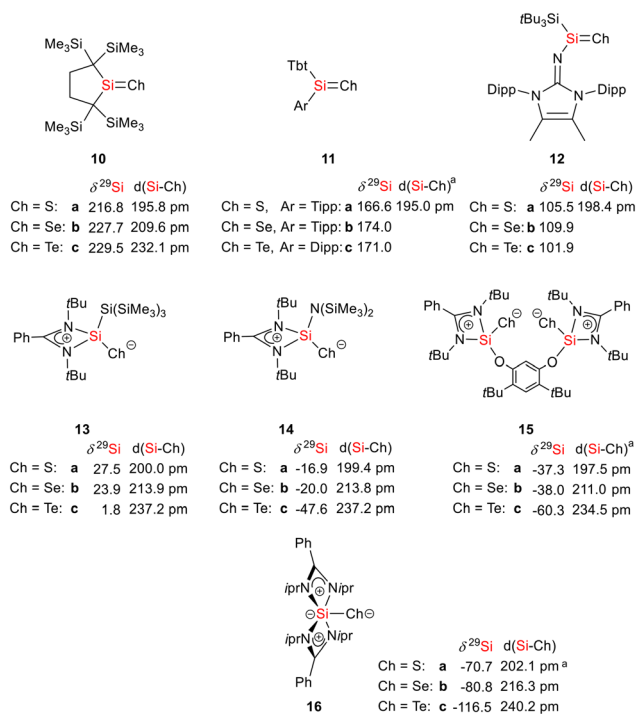
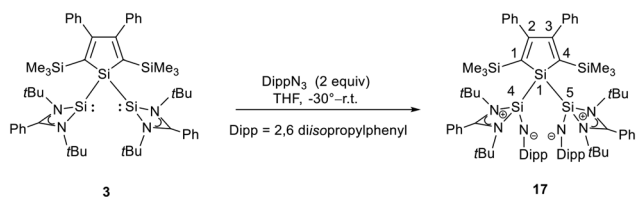


Fig. 5 Selected structural and NMR parameters of silicon chalcogenides with the silicon atom in the coordination number 3–5 (^a mean values).



Scheme 3 Reaction of bis(silylene)silole **3** with 2,6-diisopropylphenylazide.

quencies compared to the tricoordinated analogues **11b** ($\delta^{77}\text{Se} = 635$) and **11c** ($\delta^{125}\text{Te} = 731$).³⁷ Relative to typical tetracoordinated silicon selenides and tellurides such as **14b,c** ($\delta^{77}\text{Se} = -451$, $\delta^{125}\text{Te} = -1093$)³³ and **15b,c** ($\delta^{77}\text{Se} = -514$, $\delta^{125}\text{Te} = -1242$)³⁰ it is however significantly shifted to high frequencies. Although the ^{77}Se and ^{125}Te NMR chemical shift data for silicon chalcogenides in different coordination states are widely spread over large chemical shift ranges ($\delta^{77}\text{Se} = -535$ to $+635$; $\delta^{125}\text{Te} = -1236$ to $+731$), the here reported data are consistent as ^{77}Se and ^{125}Te NMR chemical shifts for this class of compounds are almost linearly correlated including compounds **8** and **9** from the present study (see the ESI† for more detailed data).⁴⁰

Sc-XRD analysis of suitable crystals of silicon chalcogenides **7**, **8** and **9** (Fig. 6) revealed molecular structures that are close to that of the bis(silylene)silole **3**. In all three cases, the central Si1Si4Si5 planes are oriented almost orthogonally to the silole ring. The increase of the coordination number of the silicon atoms Si4 and Si5 by oxidation of the bis(silylene)silole **3** resulted in slightly shorter Si1–Si4/5 bonds in the chalcogenides **7–9** (Si1–Si4/5 = 240–241 pm) compared to those in the bis(silylene) **3**. These bonds are however still long compared to the regular bonds between tetracoordinated silicon atoms (Si–Si^{mean} = 235.8 pm). All three silicon chalcogenides **7–9** show an *anti*-orientation of the chalcogen substituents relative to the central Si4–Si1–Si5 plane. The lengths of the silicon chalcogen bonds (**7**: Si–S = 199–200 pm; **8**: Si–Se = 213–214 pm; **9**: Si–Te = 237 pm) are in the typical range for tetracoordinated silicon chalcogenides (e.g. **13–15**, Fig. 5),^{24,30,33} and are placed between those reported for tricoordinated (e.g. **10** and **11**)^{34,35} and pentacoordinated silicon chalcogenides (e.g. **16**).³¹ As a result of the high polarity of the Si–Ch bonds and significant contributions from negative hyperconjugation, these bonds are all short, close to the theoretically expected value for Si=Ch double bonds (Si=S = 201 pm; Si=Se = 214 pm; Si=Te = 235 pm).^{30,32} A short discussion of the bonding of the Si–S linkage in compounds **7** and **10(S)** (for comparison) support-

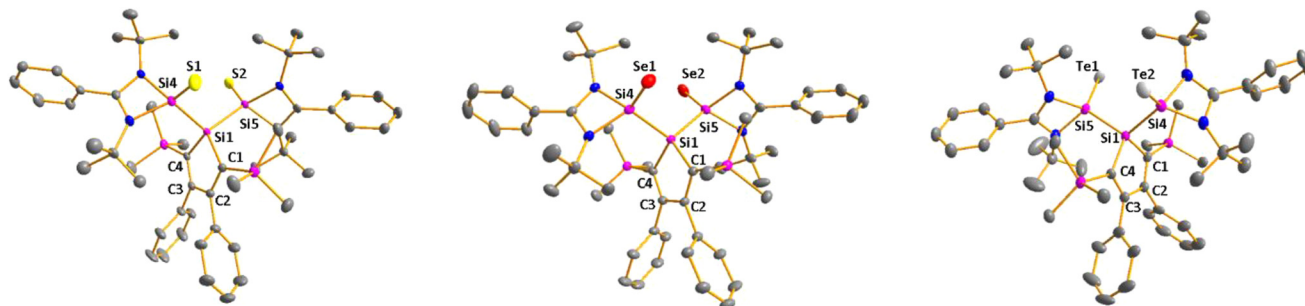


Fig. 6 Molecular structure of bis(silylene)sulphide **7** (left), bis(silylene)selenide **8** (middle) and bis(silylene)telluride **9** (right) in the crystal (hydrogen atoms are omitted; thermal ellipsoids at 50% probability). Selected atom distances [pm] and angles [°]: **7** Si1–Si4 239.19(7), Si1–Si5 239.76(6), Si4–Si1 199.33(7), Si5–S2 199.58(7), Si1–C1 188.85(20), Si1–C4 189.34(15), C1–C2 136.41(27), C2–C3 149.48(24), C3–C4 136.68(24), Si4–Si1–Si5 117.89(2); **8** Si1–Si4 239.59(7), Si1–Si5 239.98(6), Si4–Se1 213.29(7), Si5–Se2 213.61(6), Si1–C1 188.94(13), Si1–C4 189.00(12), C1–C2 136.67(16), C2–C3 149.65(16), C3–C4 136.22(18), Si4–Si1–Si5 119.51(19); **9** Si1–Si4 241.14(12), Si1–Si5 241.62(13), Si4–Te1 237.12(11), Si5–Te2 236.85(11), Si1–C1 189.43(38), Si1–C4 189.38(36), C1–C2 136.29(52), C2–C3 149.86(46), C3–C4 136.08(54), Si4–Si1–Si5 118.98(5).



ing the use of ylidic Lewis representations is provided in the ESI (pp. 30–32†).

The bissilimine **17** is formed by the reaction of two equivalents of diisopropylphenylazide, DippN₃, with bissilylene **3** in THF in 71% yield (Scheme 3). It is soluble in aromatic hydrocarbons, ethers and chlorinated hydrocarbons. Crystals suitable for sc-XRD analysis were obtained from benzene solution. The ²⁹Si{¹H} NMR spectra of bissilimine **17** display three signals at $\delta^{29}\text{Si} = -9.0$ (SiMe₃), -20.3 (silole Si), and -73.1 (imide Si). The imide silicon nuclei are significantly shielded compared to those of silaimides with tricoordinated silicon atoms (Fig. 7, cpds **18–20**).^{41,42} Its ²⁹Si NMR signal is even at the low frequency end of the typical region for tricoordinated silaguanidinium derivatives **21** and **22**^{43,44} and of tetracoordinated amidinate stabilized silicon imides (Fig. 7, cpds **23–25**).^{44,45} Interestingly, the trimethylsilyl groups of the silole ring show at room temperature in the ¹H NMR spectrum extreme line broadening (¹H NMR line width at half height: $\omega \approx 300$ Hz), indicating the steric overloading of the silaimine **17**. Crystals suitable for sc-XRD analysis were obtained from benzene solution. The molecular structure of bissilimine **17** is of C₂-symmetry with the consequence that both silaimine units have the same metrics (Fig. 8). Its main features (localized silole ring, almost orthogonally oriented silole ring and Si4/Si1/Si5 plane) are very similar to the structures of the bis-chalcogenides **7–9**. The central Si1–Si4/Si5 bonds (245.4 pm) are of the same length as in the bissilylene **3**. The Si4–N1/Si5–N2 bonds are short (159.8 pm) and compare very well with

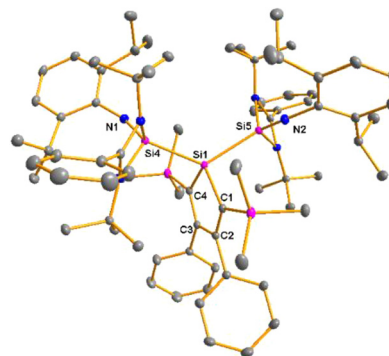


Fig. 8 Molecular structure of bissilimine **17** in the crystal (hydrogen atoms are omitted; thermal ellipsoids at 50% probability). Selected atom distances [pm] and angles [°]: Si1–Si4 245.42(4), Si4–N1 159.83(6), Si1–C1 190.08(6), C1–C2 136.97(9), C2–C3 149.96(8), Si4–Si1–Si5 125.76 (14), Si1–Si4–N1 156.16(6), Si4–N1–C^{*ipso*} 166.16(2).

those of silaimines with tricoordinated and tetracoordinated silicon atoms (Fig. 7). The Si4–N1–C^{*ipso*}/Si5–N2–C^{*ipso*} bond angles (166.2°) are wider than are usually found for *N*-aryl/alkyl substituted silaimines (*e.g.* cpds **19** and **24**) and approach the values found for *N*-silyl substituted silaimines (Fig. 7).^{42,45,46}

Conclusions

A 1,1-bisamidinosilylene-silole **3** has been synthesized and characterized. In contrast to other 1,1-disubstituted siloles with a similar substitution pattern such as **4** and **5**, bissilylene silole **3** is strongly coloured due to a bathochromic shift of the HOMO/LUMO transition. The nature of the long-wave absorption band changes from the regular $\pi(\text{silole})/\pi^*(\text{silole})$ transition of the butadiene parts of siloles **4** and **5**^{26,29} to a $\text{lp}(\text{Si})/\pi^*(\text{silole})$ transition in bissilylene silole **3** with a smaller energy separation. The stabilization of the LUMO due to more enhanced σ^*/π^* conjugation also contributes to the smaller HOMO/LUMO gap in silole **3**. Although the distance between the molecular structure of the bissilylenesilole **3** is 400 pm, close to Si/Si distances in related bissilylenes **A–E** and **G–J** (Fig. 1), we noticed no cooperative reactivity of the two nucleophilic silicon centres. We attribute this lack of cooperativity in silole **3** to the very unfavourable *anti*-orientation of the silicon lone pairs in its conformational ground state in combination with the high steric crowding around the central Si4–Si1–Si5 unit which hinders the adoption by bissilylene **3** of a conformation that is more prone to cooperative interactions between the two silicon lone pairs. Bissilylene silole **3** can be easily oxidized by elemental chalcogenides (S, Se, and Te) and by reaction with Dipp-azide. The obtained amidinato silicon chalcogenides **7–9** and the amidinato silaimine **17** adopt structures that are typical for tetracoordinated amidinato silicon derivatives with short silicon chalcogen and silicon nitrogen bonds due to their high polarity and partial double bond character due to hyperconjugation.

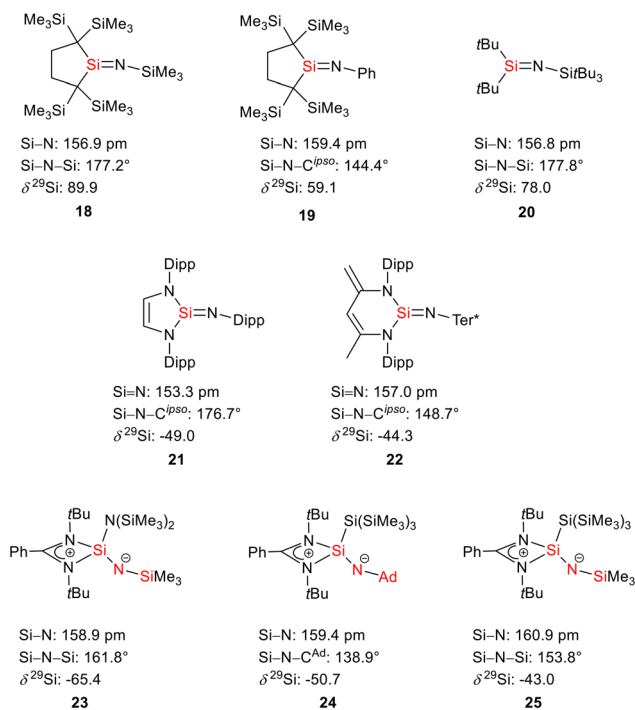


Fig. 7 Silaimines and silaguanidines with tricoordinated and tetracoordinated silicon atoms and dicoordinated nitrogen atoms (selected atom distances [pm] and angles [°]).



Author contributions

Investigation, data curation, formal analysis, validation: C. L.; conceptualization, writing, visualization, funding acquisition: C. L. and T. M.; project administration, supervision, methodology, resources: T. M.; XRD: M. S.

Conflicts of interest

There are no conflicts to declare.

Acknowledgements

This work was supported by the Deutsche Forschungsgemeinschaft (DFG) (MU-1440/13 and INST 184/227-1). Computations were done at the HPC Cluster CARL, University of Oldenburg, funded by the DFG (INST 184/108-1 FUGG) and the Ministry of Science and Culture (MWK) of the Lower Saxony State. C. L. thanks the China Scholarship Council for support CSC no.: 202108330061.

Notes and references

- 1 K. Tamao, M. Uchida, T. Izumizawa, K. Furukawa and S. Yamaguchi, Silole Derivatives as Efficient Electron Transporting Materials, *J. Am. Chem. Soc.*, 1996, **118**, 11974–11975.
- 2 Z. Zhao, B. He and B. Z. Tang, Aggregation-induced emission of siloles, *Chem. Sci.*, 2015, **6**, 5347–5365.
- 3 C.-W. So, H. W. Roesky, J. Magull and R. B. Oswald, Synthesis and Characterization of $[\text{PhC}(\text{NtBu})_2]\text{SiCl}$: A Stable Monomeric Chlorosilylene, *Angew. Chem., Int. Ed.*, 2006, **45**, 3948–3950.
- 4 M. Nazish, C. M. Legendre, R. Herbst-Irmer, S. Muhammed, P. Parameswaran, D. Stalke and H. W. Roesky, Synthesis and Characterization of Substituted Phosphasilenes and its Rare Homologue Stibasilene $>\text{Si}=\text{Sb}-$, *Chem. – Eur. J.*, 2023, **29**, e202300791.
- 5 M. Nazish, C. M. Legendre, N. Graw, R. Herbst-Irmer, D. Stalke, S. Sankar Dutta, U. Lourderaj and H. W. Roesky, Coordination and Stabilization of a Lithium Ion with a Silylene, *Chem. – Eur. J.*, 2023, **29**, e202203528.
- 6 S. S. Sen, H. W. Roesky, D. Stern, J. Henn and D. Stalke, High Yield Access to Silylene RSiCl ($\text{R} = \text{PhC}(\text{NtBu})_2$) and Its Reactivity toward Alkyne: Synthesis of Stable Disilacyclobutene, *J. Am. Chem. Soc.*, 2010, **132**, 1123–1126.
- 7 Z. Hendi, M. K. Pandey, K. Rachuy, M. K. Singh, R. Herbst-Irmer, D. Stalke and H. W. Roesky, Synthesis, Reactivity, and Complexation with $\text{Fe}(0)$ of a Tight-bite *Bis*(N-heterocyclic silylene), *Chem. – Eur. J.*, 2024, e202400389.
- 8 J. Xu, S. Pan, S. Yao, G. Frenking and M. Driess, The Heaviest Bottleable Metallylone: Synthesis of a Monatomic, Zero-Valent Lead Complex (“Plumbylone”), *Angew. Chem., Int. Ed.*, 2022, **61**, e202209442.
- 9 Y. Xiong, S. Dong, S. Yao, J. Zhu and M. Driess, Unexpected White Phosphorus (P_4) Activation Modes with Silylene-Substituted o-Carboranes and Access to an Isolable 1,3-Diphospha-2,4-disilabutadiene, *Angew. Chem., Int. Ed.*, 2022, **61**, e202205358.
- 10 X. Chen, H. Wang, S. Du, M. Driess and Z. Mo, Deoxygenation of Nitrous Oxide and Nitro Compounds Using *Bis*(N-Heterocyclic Silylene)Amido Iron Complexes as Catalysts, *Angew. Chem., Int. Ed.*, 2022, **61**, e202114598.
- 11 Y. Xiong, S. Dong, S. Yao, C. Dai, J. Zhu, S. Kemper and M. Driess, An Isolable 2,5-Disila-3,4-Diphosphapyrrole and a Conjugated $\text{Si}=\text{P}=\text{Si}=\text{P}=\text{Si}=\text{N}$ Chain Through Degradation of White Phosphorus with a *N,N-Bis*(Silylenyl)Aniline, *Angew. Chem., Int. Ed.*, 2022, **61**, e202209250.
- 12 S. Yao, A. Kostenko, Y. Xiong, C. Lorent, A. Ruzicka and M. Driess, Changing the Reactivity of Zero- and Mono-Valent Germanium with a Redox Non-Innocent *Bis*(silylenyl)carborane Ligand, *Angew. Chem., Int. Ed.*, 2021, **60**, 14864–14868.
- 13 S. Yao, T. Szilvási, Y. Xiong, C. Lorent, A. Ruzicka and M. Driess, *Bis*(silylene)-Stabilized Monovalent Nitrogen Complexes, *Angew. Chem., Int. Ed.*, 2020, **59**, 22043–22047.
- 14 W. Wang, S. Inoue, S. Yao and M. Driess, An Isolable *Bis*-Silylene Oxide (“Disilylenoxane”) and Its Metal Coordination, *J. Am. Chem. Soc.*, 2010, **132**, 15890–15892.
- 15 D. Gallego, S. Inoue, B. Blom and M. Driess, Highly Electron-Rich Pincer-Type Iron Complexes Bearing Innocent *Bis*(metallylene)pyridine Ligands: Syntheses, Structures, and Catalytic Activity, *Organometallics*, 2014, **33**, 6885–6897.
- 16 Y. Wang, A. Kostenko, S. Yao and M. Driess, Divalent Silicon-Assisted Activation of Dihydrogen in a *Bis*(N-heterocyclic silylene)xanthene Nickel(0) Complex for Efficient Catalytic Hydrogenation of Olefins, *J. Am. Chem. Soc.*, 2017, **139**, 13499–13506.
- 17 Y.-P. Zhou, S. Raoufmoghaddam, T. Szilvási and M. Driess, A *Bis*(silylene)-Substituted ortho-Carborane as a Superior Ligand in the Nickel-Catalyzed Amination of Arenes, *Angew. Chem., Int. Ed.*, 2016, **55**, 12868–12872.
- 18 W. Wang, S. Inoue, S. Enthaler and M. Driess, *Bis*(silylenyl)- and *Bis*(germylenyl)-Substituted Ferrocenes: Synthesis, Structure, and Catalytic Applications of Bidentate Silicon(II)–Cobalt Complexes, *Angew. Chem., Int. Ed.*, 2012, **51**, 6167–6171.
- 19 W. Wang, S. Inoue, E. Irran and M. Driess, Synthesis and Unexpected Coordination of a Silicon(II)-Based SiCSi Pincerlike Arene to Palladium, *Angew. Chem., Int. Ed.*, 2012, **51**, 3691–3694.
- 20 H.-X. Yeong, H.-W. Xi, Y. Li, K. H. Lim and C.-W. So, A Silyliumylidene Cation Stabilized by an Amidinate Ligand and 4-Dimethylaminopyridine, *Chem. – Eur. J.*, 2013, **19**, 11786–11790.
- 21 S. K. Kushvaha, P. Kallenbach, S. M. N. V. T. Gorantla, R. Herbst-Irmer, D. Stalke and H. W. Roesky, Preparation of a Compound with a $\text{Si}^{\text{II}}-\text{Si}^{\text{IV}}-\text{Si}^{\text{II}}$ Bonding Arrangement, *Chem. – Eur. J.*, 2024, **30**, e202303113.



- 22 A. Bande and J. Michl, Conformational Dependence of σ -Electron Delocalization in Linear Chains: Permethylated Oligosilanes, *Chem. – Eur. J.*, 2009, **15**, 8504–8517.
- 23 Z. Dong, C. R. W. Reinhold, M. Schmidtman and T. Müller, Trialkylsilyl-Substituted Silole and Germole Dianions, *Organometallics*, 2018, **37**, 4736–4743.
- 24 M. K. Bisai, V. S. V. S. N. Swamy, T. Das, K. Vanka, R. G. Gonnade and S. S. Sen, Synthesis and Reactivity of a Hypersilylsilylene, *Inorg. Chem.*, 2019, **58**, 10536–10542.
- 25 C. R. W. Reinhold, Z. Dong, J. M. Winkler, H. Steinert, M. Schmidtman and T. Müller, A One-Step Germole to Silole Transformation and a Stable Isomer of a Disilabenzene, *Chem. – Eur. J.*, 2018, **24**, 848–854.
- 26 S. Yamaguchi, R.-Z. Jin and K. Tamao, Modification of the electronic structure of silole by the substituents on the ring silicon, *J. Organomet. Chem.*, 1998, **559**, 73–80.
- 27 The Gaussian 16 program was used, see the ESI† for details.
- 28 A. Pöcheim, G. A. Özpınar, T. Müller, J. Baumgartner and C. Marschner, The Combination of Cross-Hyperconjugation and σ -Conjugation in 2,5-Oligosilyl Substituted Siloles, *Chem. – Eur. J.*, 2020, **26**, 17252–17260.
- 29 S. Yamaguchi and K. Tamao, Silole-containing σ - and π -conjugated compounds, *J. Chem. Soc., Dalton Trans.*, 1998, 3693–3702, DOI: [10.1039/A804491K](https://doi.org/10.1039/A804491K).
- 30 M. Ghosh, P. Panwaria, S. Tothadi, A. Das and S. Khan, Bis(silanetellurone) with C–H...Te Interaction, *Inorg. Chem.*, 2020, **59**, 17811–17821.
- 31 K. Junold, J. A. Baus, C. Burschka, D. Auerhammer and R. Tacke, Stable Five-Coordinate Silicon(IV) Complexes with SiN_4X Skeletons (X=S, Se, Te) and $\text{Si}=\text{X}$ Double Bonds, *Chem. – Eur. J.*, 2012, **18**, 16288–16291.
- 32 D. Lutters, A. Merk, M. Schmidtman and T. Müller, The Silicon Version of Phosphine Chalcogenides: Synthesis and Bonding Analysis of Stabilized Heavy Silaldehydes, *Inorg. Chem.*, 2016, **55**, 9026–9032.
- 33 Y.-C. Chan, Y. Li, R. Ganguly and C.-W. So, Acyclic Amido-Containing Silanechalcogenones, *Eur. J. Inorg. Chem.*, 2015, 3821–3824.
- 34 T. Iwamoto, K. Sato, S. Ishida, C. Kabuto and M. Kira, Synthesis, Properties, and Reactions of a Series of Stable Dialkyl-Substituted Silicon–Chalcogen Doubly Bonded Compounds, *J. Am. Chem. Soc.*, 2006, **128**, 16914–16920.
- 35 H. Suzuki, N. Tokitoh, S. Nagase and R. Okazaki, The First Genuine Silicon-Sulfur Double-Bond Compound: Synthesis and Crystal Structure of a Kinetically Stabilized Silanethione, *J. Am. Chem. Soc.*, 1994, **116**, 11578–11579.
- 36 H. Suzuki, N. Tokitoh, R. Okazaki, S. Nagase and M. Goto, Synthesis, Structure, and Reactivity of the First Kinetically Stabilized Silanethione, *J. Am. Chem. Soc.*, 1998, **120**, 11096–11105.
- 37 N. Tokitoh, T. Sadahiro, K. Hatano, T. Sasaki, N. Takeda and R. Okazaki, Synthesis of Kinetically Stabilized Silaneselone and Silanetellone, *Chem. Lett.*, 2002, **31**, 34–35.
- 38 A. V. Protchenko, P. Vasko, D. C. H. Do, J. Hicks, M. Á. Fuentes, C. Jones and S. Aldridge, Reduction of Carbon Oxides by an Acyclic Silylene: Reductive Coupling of CO, *Angew. Chem., Int. Ed.*, 2019, **58**, 1808–1812.
- 39 H. Zhu, F. Hanusch and S. Inoue, Facile Bond Activation of Small Molecules by an Acyclic Imino(silyl)silylene, *Isr. J. Chem.*, 2023, **63**, e202300012.
- 40 Correlation between ^{77}Se and ^{125}Te compounds of equivalent compounds, see: H. C. E. McFarlane and W. McFarlane, *J. Chem. Soc., Dalton Trans.*, 1973, 2416–2418.
- 41 N. Wiberg, K. Schurz and G. Fischer, Isolation of the Stable Silaketimine $t\text{Bu}_2\text{Si}=\text{N}-\text{Si}t\text{Bu}_3$, *Angew. Chem., Int. Ed. Engl.*, 1985, **24**, 1053–1054.
- 42 T. Iwamoto, N. Ohnishi, Z. Gui, S. Ishida, H. Isobe, S. Maeda, K. Ohno and M. Kira, Synthesis and structure of stable base-free dialkylsilanimines, *New J. Chem.*, 2010, **34**, 1637–1645.
- 43 L. Kong and C. Cui, Synthesis and Reactivity of a Base-Free N-Heterocyclic Silanimine, *Organometallics*, 2010, **29**, 5738–5740.
- 44 P. P. Samuel, R. Azhakar, R. S. Ghadwal, S. S. Sen, H. W. Roesky, M. Granitzka, J. Matussek, R. Herbst-Irmer and D. Stalke, Stable Silanimines with Three- and Four-Coordinate Silicon Atoms, *Inorg. Chem.*, 2012, **51**, 11049–11054.
- 45 M. K. Bisai, V. Sharma, R. G. Gonnade and S. S. Sen, Reactivities of Silanimines with Boranes: From Cooperative B–H Bond Activation to Donor Stabilized Silyl Cation, *Organometallics*, 2021, **40**, 2133–2138.
- 46 N. Wiberg and K. Schurz, Zur Kenntnis des stabilen Silanimins $t\text{Bu}_2\text{Si}=\text{N}-\text{Si}t\text{Bu}_3$ und seiner Donoraddukte, *Chem. Ber.*, 1988, **121**, 581–589.

